Mesoporous methyl-functionalized Sn-silicates generated by the aerosol process for the sustainable production of ethyl lactate

Alvise Vivian[†], Luca Fusaro[†], Damien P. Debecker[‡,], Carmela Aprile[†,*]*

[†] University of Namur, Department of Chemistry, Unit of Nanomaterials Chemistry, 5000 Namur, Belgium

[‡] UCLouvain, Institute of Condensed Matter and Nanoscience, 1348 Louvain-la-Neuve, Belgium.

*Corresponding authors: carmela.aprile@unamur.be ; damien.debecker@uclouvain.be

Abstract

The aerosol-assisted sol-gel process was used to synthesize in a straightforward one-pot procedure a series of methyl-functionalized tin silicates with different degrees of methylation. The successful incorporation of isolated Sn as single site within the silica framework was confirmed via ^{119}Sn Solid State NMR measurements, while ^{29}Si and ^{13}C solid-state magic-angle-spinning NMR experiments revealed a degree of methylation close to the theoretical value, hence proving the efficacy of the adopted co-synthetic approach. These materials were tested as catalysts in the synthesis of ethyl lactate from dihydroxyacetone and ethanol. The methylated solids display enhanced performances in terms of both activity and selectivity compared to the non-methylated analogues, highlighting a strong beneficial role of surface hydrophobicity. Under proper conditions a total conversion and a selectivity higher than 95% were achieved. Moreover, the

efficient separation and reuse of the heterogeneous catalyst as well as the possibility of an easily recover of the reaction solvent result in a very low waste production protocol with an exceptionally low E-factor.

Keywords

Mesoporous mixed oxide; hybrid materials; hydrophobicity; biorefinery; spray drying

Introduction

One of the main challenges of our century is the development of more sustainable chemical processes in agreement with the 12 Principles of Green Chemistry established by Anastas and Warner.[1] To cope with these sustainability principles, catalysis scientists have a central role to play for the development of processes based on the utilization of renewable feedstocks, run under mild conditions, using harmless solvent or no solvent, and achieving high atom-economy.[2] In the panorama of bio-based renewable supply, lignocellulose is considered the most abundant source available for the production of fuels and chemicals in the biorefinery.[3,4]

Recently lactic acid and alkyl lactates attracted a considerable interest from both academic and industrial parties for the broad window of possible applications ranging from green solvents and intermediates for the production of pharmaceutical and cosmetic products.[5–9] Moreover, lactates are precursors for the synthesis of lactide and polylactates, used for the synthesis of biodegradable plastic materials.[10–15]

Several feedstocks have been used as carbohydrate sources for the production of lactic acid and alkyl lactates including cellulose, glucose, fructose and trioses.[16] The last step of the complex series of transformation leading to the synthesis of ethyl lactate (EL) from cellulose (Scheme 1) is represented by the conversion of dihydroxyacetone (DHA). This reaction can be classified as a high atom economy process (87%) with a potentially low E factor.[17] In 2005 homogeneous Sn halide catalysts were used for the first time in the conversion of sugars to lactates.[18] Since then, increasing efforts were directed towards the development of heterogeneous catalytic systems to further improve the sustainability of the process. More

recently, a remarkable number of Sn-based heterogeneous catalyst were reported for the conversion of trioses to alkyl lactates, including zeolites (MFI, USY, Beta),[19–22] Sn-MCM-41,[23–26] and silica-carbon composites.[25] Recently, we proposed a new class of mesoporous Sn-silicate microparticles obtained via the aerosol-assisted sol-gel process, which exhibited record activity in the conversion of DHA to ethyl lactate.[27]

In order to achieve high activity and selectivity, with associated reduction of by-products and wastes, various parameters can be optimized including catalysts textural properties, thermal and chemical stability, nature and dispersion of the active sites, acidity and basicity. However, another important and often underestimated parameter is represented by the hydrophilic/hydrophobic balance of the catalyst surface. The latter dictates the interaction in the adsorption and desorption steps between the catalytic material and the reagents, products and by-products, influencing in this way the catalytic performance. The hydrophilic character of silica-based solids, due to the presence of surface silanol groups, can be modified by alkylation procedures using co-synthetic or post-grafting strategies. In the context of alkyl lactate production from DHA, it was hypothesized by Lari and coworkers[28] that the lower interaction of water with the surface of hydrophobic Sn-MFI and Sn-BEA zeolites favors a displacement of the dehydration equilibrium towards the pyruvic aldehyde (PA) intermediate, hence improving the DHA conversion and the selectivity. However, to the best of our knowledge, a systematic investigation of role played by the hydrophobic/hydrophilic properties of the catalyst surface on the conversion of DHA to alkyl lactates was never performed.

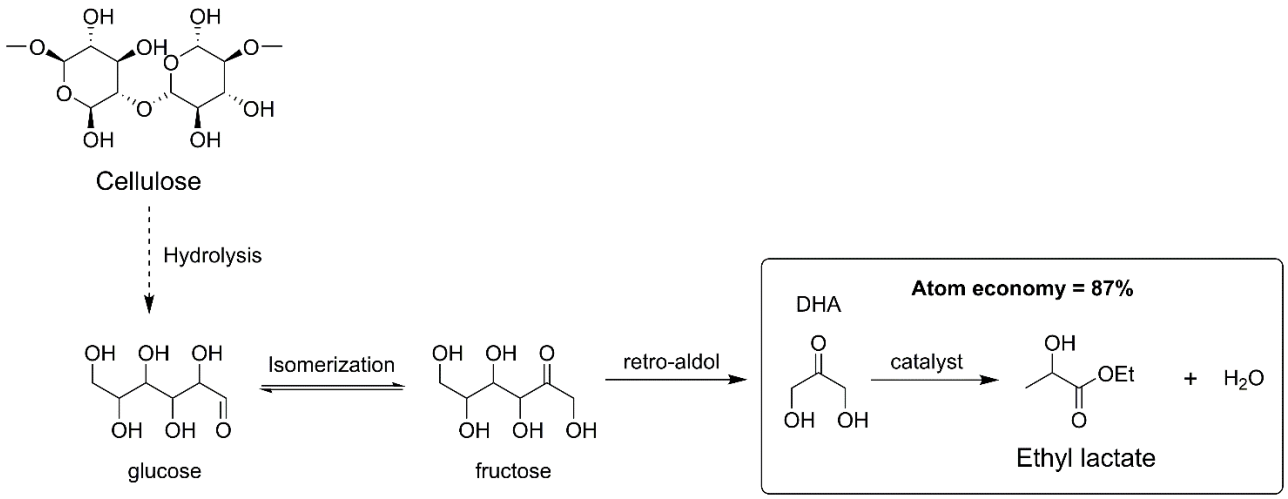

Scheme 1. Acid-catalyzed reaction scheme for the production of ethyl lactate from DHA, hexoses or polysaccharides

As reviewed recently,[29] aerosol processes have already been applied for the production of several metallosilicate materials exhibiting excellent catalytic performance in various chemical reactions, like for example SiAl oxides for hydrocarbon cracking,[30] SiMoAl oxides and SiW oxides for olefin metathesis,[31–33] SiTi oxides for selective oxidation,[34,35] etc. In these preparation procedures, a precursors solution containing a texturing agent is sprayed and processed (dried) under mild temperature to rapidly trigger the inorganic polycondensation reactions, yielding materials with spherical shape, high homogeneity and tunable texture. These processes have been coined as "Type IIIc" aerosol processes in a recently proposed classification.[29] The advantages of this process compared to conventional sol-gel approaches include: a limited number of steps, a much shorter synthesis time, a limited waste generation and low environmental impact.[36,37] Moreover, the catalyst preparation process can be scaled up easily and can be run in a continuous mode, making it industrially attractive. Recently, the preparation of hybrid catalysts via such aerosol process has been reported, including materials based on periodic mesoporous organosilica (PMO)[38] and metal organic framework (MOF).[39] Yet the preparation of surface functionalized metallosilicate catalysts has not been reported to date.

Herein, we take advantage of the highly versatile aerosol-assisted sol-gel process to synthesize, in a one-pot procedure, of a novel class of methyl-functionalized tin silicates with different degrees of methylation. Tuning the hydrophilic/hydrophobic character of the catalyst surface is presented as a method to further boost the catalytic performance of these formulations in the conversion of dihydroxyacetone to ethyl lactate.

Results and Discussion

Two series of Sn-silicates with different degrees of methyl (Me) functionalities were synthesized using the aerosol-assisted sol-gel process in one-pot co-synthetic approach selecting a Si/Sn atomic ratio of 74.[27]

To that end, an aqueous-ethanolic precursor solution containing tin(IV) tetrachloride pentahydrate, tetraethylorthosilicate (TEOS), and methyltriethoxysilane (MTES) – as the source of methyl groups – was atomized and rapidly dried in a tubular furnace set at 350°C. It must be mentioned that the reproducibility of the synthesis is strongly related to the careful control of all the synthesis parameters (e.g. temperature, pre-hydrolysis time of the precursors, working parameters of the aerosol setup, etc.). Initially, porous Sn-based solids with a low degree of methylation (2 and 5%$_{mol}$) were synthesized. The influence of two structure-directing agents from the Pluronic family (F127 and P123) on the morphological properties of the materials was studied as well. The materials were denoted as Sn-x-F127 and Sn-x-P123 (where x indicates the nominal percentage of methylation, i.e. the molar MTES / (MTES + TEOS) x 100 % ratio).

In order to investigate the effect of a higher amount of methyl moieties, two additional solids bearing a theoretical methylation degree of 10 and 30%$_{mol}$ were prepared. For this investigation Pluronic F127 was selected as templating agent.

The as-synthesized materials were analyzed by quantitative solid state ^{29}Si MAS (magic-angle-spinning) NMR investigation, revealing that the methylation degree was always close to the theoretical value for all solids (see SI, Figure S1 and Table S1).

The templating agent has to be removed to release the porosity, while preserving the organic-functionalization. Several procedures have been reported in literature for the removal of Pluronics from as-synthesized nanomaterials, including solvent extraction[40] or calcination.[41] Different solvent extraction procedures, including the one reported by Zhao *et al.*[42] were initially considered. However, under the selected conditions (Table S2) the total removal of the surfactant was not achieved and a significant template residue (around 10%$_{wt}$) was found. To overcome the incomplete removal of the surfactant obtained with the extraction technique, a mild calcination treatment was optimized taking inspiration from the work of Grudzien *et al*.[43] For this investigation the solid with the highest Me degree (Sn-30-F127) was selected as target material and a calcination screening at different temperatures was performed. The loss of both templating agent and methyl-functionalization (Figure S2a, S2b and Table S3) was followed by a combination of ^{29}Si and ^{13}C solid state MAS NMR.

The best compromise between a complete removal of the surfactant and only a minor loss of the methyl-functionalization was achieved with a thermal treatment at 250 °C for 8h. Thus, all the solids were calcined at the selected temperature and, as proved by ^{29}Si solid state MAS NMR experiments (Figure 1, Table S4), the initial amount of methyl moieties was largely preserved in all materials. Similar results were obtained with the Sn-x-P123 samples (figure S3 and Table S4), showing that the mild thermal treatment was also applicable to this texturing agent.

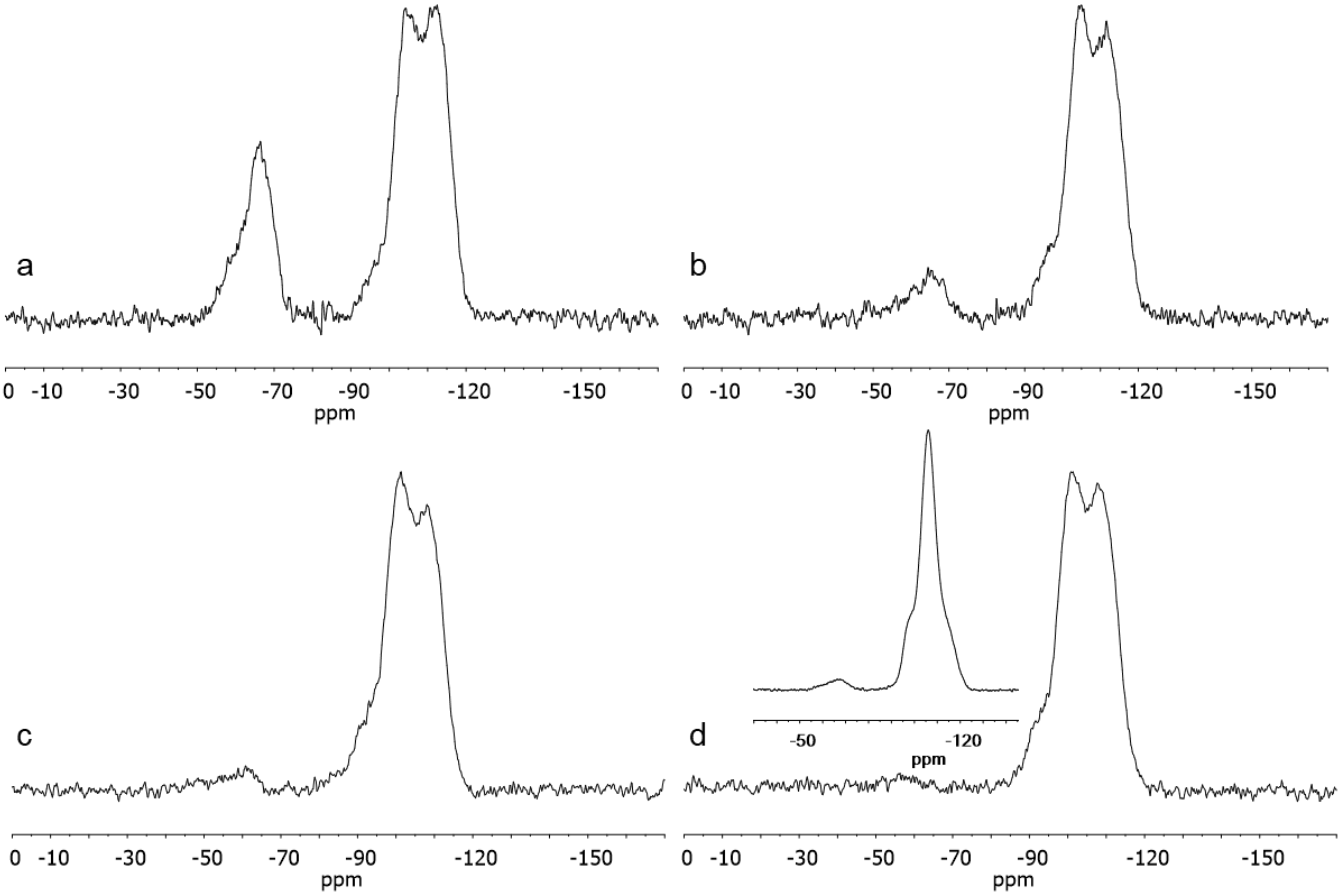

Figure 1. Solid state ^{29}Si MAS NMR spectra (direct excitation experiments) of methylated Sn-x-F127 after calcination treatment at 250 °C for 8h. Sn-30-F127 (a), Sn-10-F127 (b), Sn-5-F127 (c) and Sn-2-F127 (d) with cross-polarization experiment (inset)

Figure 1 shows the quantitative ^{29}Si direct excitation (DE) MAS spectra of the Sn-x-F127 series, the corresponding spectra of the Sn-x-P123 series can be found in supporting information (Figure S3). Clear Q^4

[$(SiO)_4Si$] (-111 ppm) and Q^3 [$(SiO)_3SiOH$] (-102 ppm) signals can be observed in all samples. The ^{29}Si spectra of methyl-functionalized solids display two peaks at −66 and −59 ppm, assigned respectively to $MeSi(OSi)_3$ (T^3) and $Me(HO)Si(OSi)_2$ (T^2) species. Due to the very low degree of functionalization in both Sn-2-F127 and Sn-2-P123, the presence of methyl groups was confirmed also by performing cross-polarization (CP) experiments (see Figure 1d (inset) and Figure S3a).

The Sn loading was quantified by inductively coupled plasma optical emission spectroscopy (ICP-OES). The experimental composition – expressed in Si/Sn ratio – was very close to the nominal composition (Table 1). The successful incorporation of Sn as isolated sites within the silica framework was confirmed via ^{119}Sn solid-state NMR. Static ^{119}Sn NMR measurement performed on calcined solids allows evidencing that Sn is inserted in tetrahedral coordination. The signal observed at around –700 ppm (Figure 2d and 2e) can be assigned to intra-framework Sn(IV) species connected to four silicon atoms via oxygen bridges or partially hydrated tin species with an extended coordination shell.[27] Similar results were obtained for all the Sn-based solids (Figure S4). This investigation allows excluding the presence of important amount of extra-framework SnO_2 species, which would yield a signal presenting a maximum at around -600 ppm (Figure S5). Therefore, even considering the broad linewidth of the signals, the presence of extra-framework SnO_2 is excluded.

In order to elucidate the influence of the thermal treatment on the incorporation of Sn, ^{119}Sn-NMR experiments were performed also on the as-synthesized samples (i.e. directly recovered from the aerosol process and before calcination). Interestingly, an evident increase of the contribution centered at -700 ppm was observed after treatment of the samples at 250°C, together with a shift of the signal toward lower frequency (Figure 2). So, it appears that the thermal treatment was of crucial importance not only for the removal of the templating agent but also to favor the transition of Sn as single site within the silica structure. For comparison and to evidence even more the transition from extra- to intra-framework tin species the solid state ^{119}Sn NMR of $SnCl_4 \cdot 5\ H_2O$ was added as well (figure 2a).

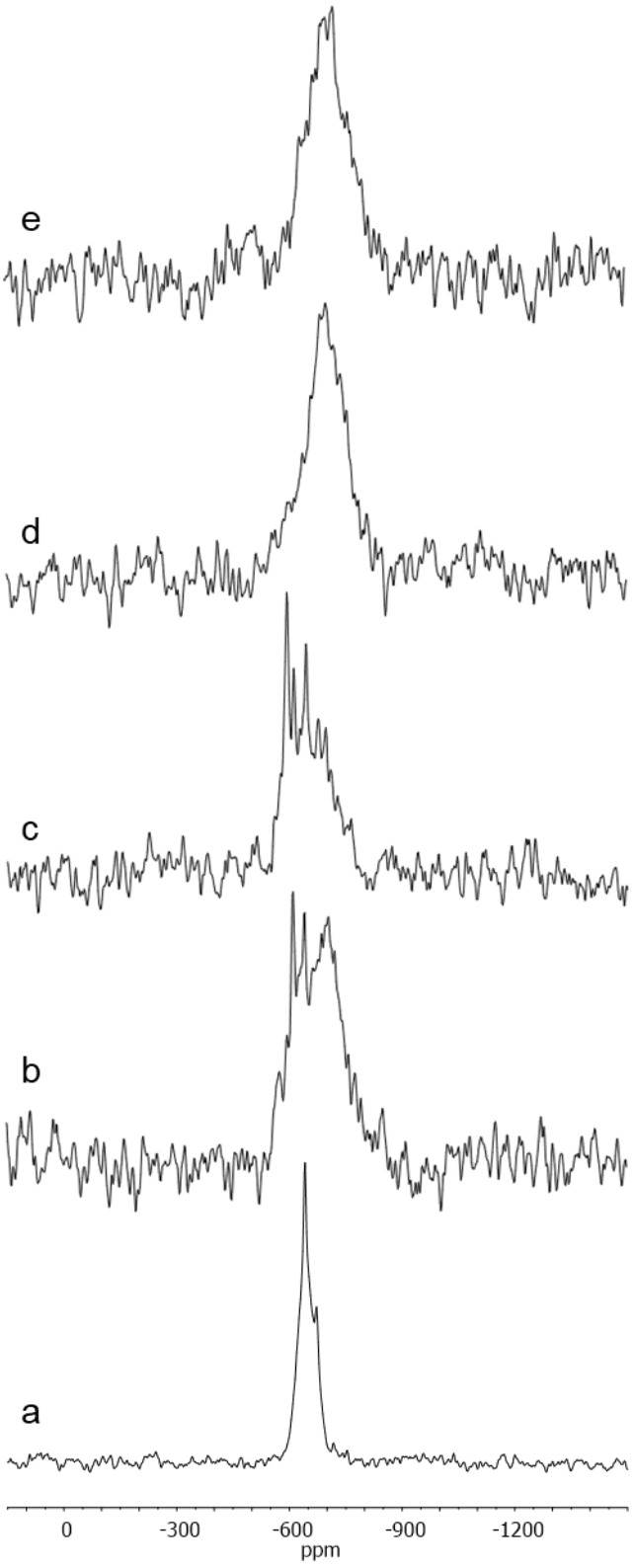

Figure 2. ^{119}Sn Static Solid State NMR of $SnCl_4 \cdot 5\ H_2O$ (a), Sn-2-P123 as-synthesized (b), Sn-2-F127 as-synthesized (c), Sn-2-P123 after calcination at 250 °C (d) and Sn-2-F127 after calcination at 250 °C (e)

The sample morphology was investigated by transmission electron microscopy (TEM). All solids displayed a spherical shape with a mesoporous structure and a pores size distribution in the 5-7 nm range. When F127 was used as a surfactant, a regular cubic mesostructured was obtained with an estimated pore diameter of 7 nm, throughout the particles, even when the organic-functionalization was raised to 30% (see Figure S6). However, the materials synthesized in the presence of P123 display a substantial deformation of the regular cubic mesostructure on the periphery of the particles (Figure 3a and 3b). This difference between the two series of solids (Sn-x-P123 and Sn-x-F127) could be explained as a function of the different hydrophilic-hydrophobic balance of the two triblock polymers. Both surfactants can be defined by the general formula "PEOxPPOyPEOx" where PPO represents the poly(propylene oxide) part and PEO stands for poly(ethylene oxide).

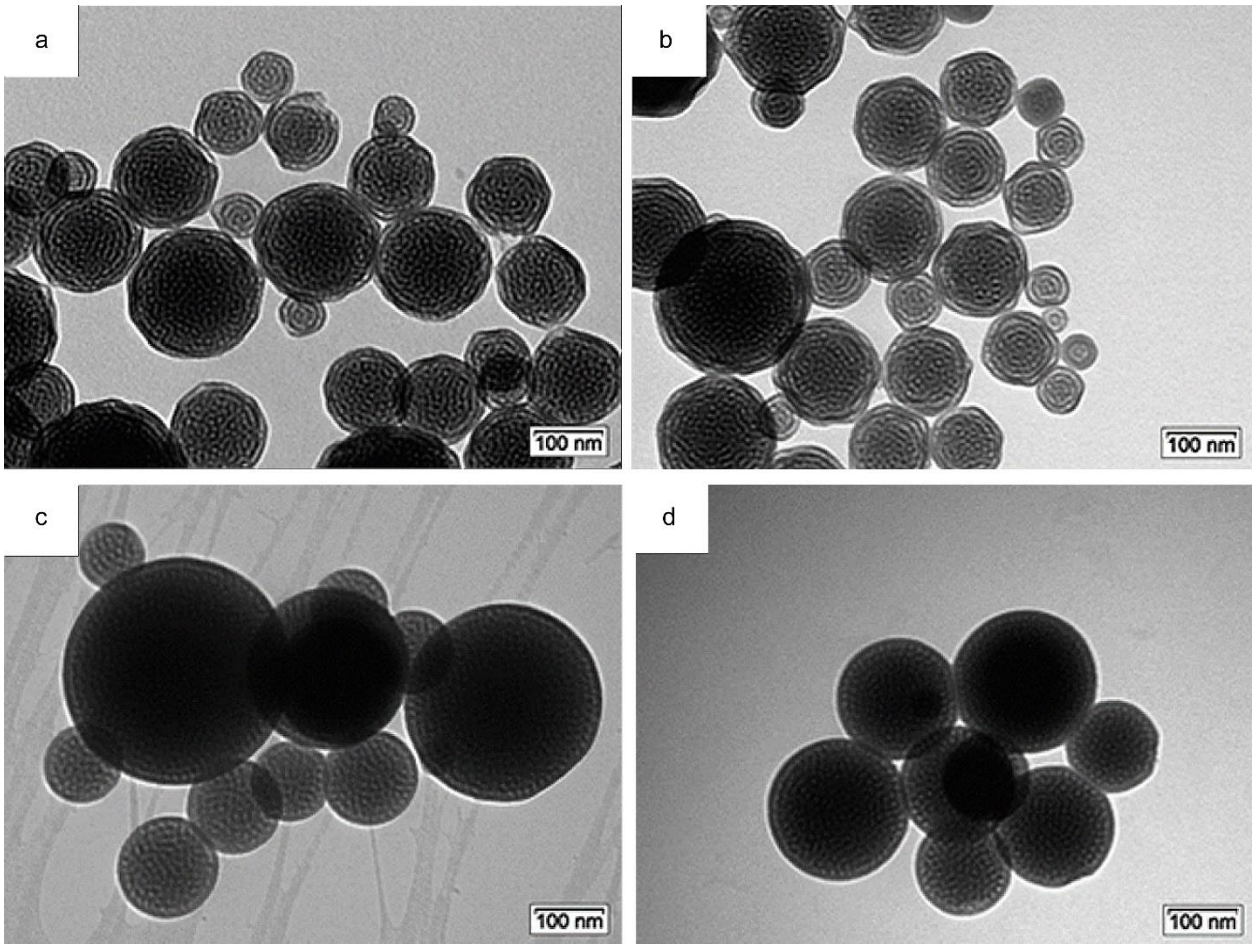

Figure 3. TEM micrographs of Sn-2-P123 (a), Sn-5-P123 (b), Sn-2-F127 (c), Sn-5-F127 (d)

In the conditions used for the synthesis of the porous solids, the central PPO block constitutes the hydrophobic core while the PEO represents the hydrophilic shell. The lower amount of hydrophilic units in the P123 may be responsible of an increased affinity with the hydrophobic methyl groups of the MTES which could be oriented toward the hydrophobic shell of the micelles causing a structural deformation of the final solid.[44] The low angle powder XRD patterns of Sn-x-P123 materials (Figure 4) featured mainly first order d_{100} diffraction peaks (with a *d*-spacing of 9 nm) typical of ordered mesostructured oxides assembled using a non-ionic surfactants, forming 'wormlike' pore channel structures.[45] Particles templated with F127 show one diffraction peak (d_{110} = 11.2 nm) consistent with a face-centered-cubic (FCC) structure.[46]

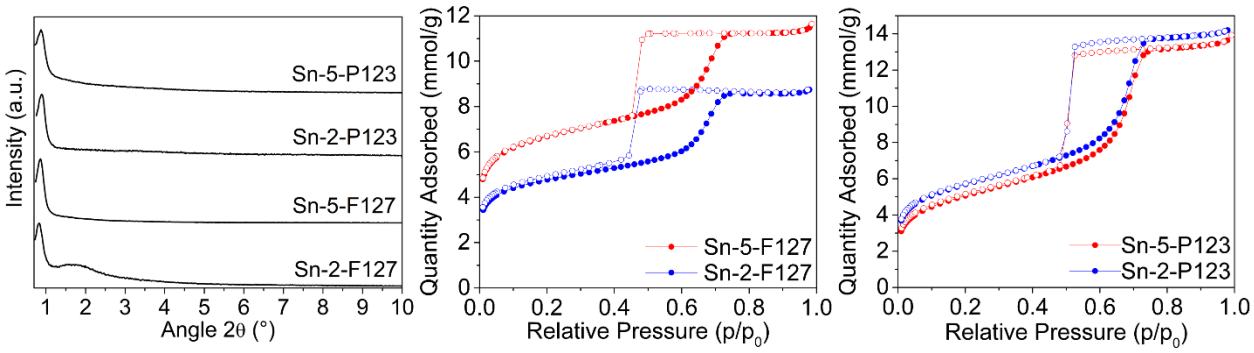

Figure 4. Nitrogen adsorption/desorption isotherms of Sn-x-F127, Sn-x-P123 solids and Small-angle XRD patterns

For both solids, N_2-physisorption measurements showed a type-IV isotherm characterized by an evident H2 hysteresis loop. In good agreement with TEM observations, the BJH analysis performed on the adsorption branch of the isotherm evidenced a narrow pore size distribution. An overview of the textural properties of methylated Sn-silicates is reported in Table 1.

Table 1. Physicochemical properties of methylated Sn-silicates

Material	BET SSA ($m^2\ g^{-1}$)	MPS[a] (nm)	BJH pore size (nm)	Pore Volume ($cm^3\ g^{-1}$)	Inter-reticular	Si/Sn[b]

					distance (nm)	
Sn-30-F127	540	160	5	0.44	11.4	71
Sn-10-F127	570	175	6.8	0.46	11.6	80
Sn-5-F127	550	185	7.0	0.41	11.9	81
Sn-2-F127	560	170	6.7	0.47	12.3	86
Sn-5-P123	470	180	6.4	0.6	9.0	77
Sn-2-P123	400	185	6.3	0.5	9.0	76

a) Mean Particle Size, b) Si/Sn determined by ICP-OES analysis

The two series of methylated Sn-silicates, displaying successful incorporation of Sn as single site in the silica matrix, high surface area and methyl moieties were tested in the synthesis of ethyl lactate from dihydroxyacetone, in ethanol (Table 2).[27] From a preliminary comparison between Sn-x-F127 and Sn-x-P123n it emerged that the solids synthesized using F127 as templating agent displayed better catalytic performances (compare entries 1 with 3 for a methylation degree of 2%, and entries 2 with 4 for a methylation degree of 5%). The lower activity of the Sn-x-P123 catalysts may be ascribed to the substantial deformation of the surface morphology observed in the presence of P123 as well as the slightly lower SSA and to the lower amount of methyl groups available at the external surface of the solids. No significant improvement in the catalyst performance was observed when the methylation degree is brought to 10% (Sn-10-F127, entry 5). An even higher content of methyl groups (30%) in the formulation leads to a lowering of the ethyl lactate yield (see entry 6). Despite the rather high selectivity, the presence of an intermediate (diethyl acetal of pyruvic aldehyde) was always observed. This can be explained considering the mechanism of the reaction (reported elsewhere[23]) as well as the combination of Brønsted and Lewis acid sites generated by isomorphic substitution of silicon with tin. However, it is worth mentioning that a total conversion with a selectivity higher than 95% can be achieved by slightly modifying the reaction conditions (*vide infra*). To verify the reproducibility of the catalytic results, the materials were tested three times under the same reaction conditions. The associated error calculated was around 2%, proving the high reproducibility of the catalytic tests.

Table 2. Catalytic activity of methylated Sn-silicate catalysts in the synthesis of ethyl lactate

Entry	Catalyst	Calc. T (°C)	Y_{EL} (%)	X_{DHA} (%)	Sel. $_{EL}$ (%)	TON[b]
1	Sn-2-P123	250	27	39	68	67
2	Sn-5-P123	250	31	42	73	74
3	Sn-2-F127	250	46	62	76	127
4	Sn-5-F127	250	50	65	76	125
5	Sn-10-F127	250	50	64	78	120
6	Sn-30-F127	250	33	47	69	90

Reaction conditions: 50 mg of catalyst, 5 mL of 0.4 M DHA solution in absolute ethanol, 6 h at 90 °C under 1200 rpm stirring. [b] TON (Turnover number) here defined as mol of DHA converted / mol of Sn after 6 h of reaction

In the light of these results, the more performing Sn-2-F127 and Sn-5-F127 materials were compared with a non-methylated analogous (Sn-0-F127) synthesized under the same conditions. The full characterization of Sn-0-F127 solid is available as supporting information (Figure S7). From this comparison emerged a positive influence of the methylation on the performances of the catalysts (compare entries 1-2 with entry 4 in table 3) both in terms of yield and selectivity. It is important to underline that even a very low degree of methylation was enough to enhance the catalytic activity of the solids.

Table 3. Catalytic activity of methylated and non-methylated Sn-silicate catalysts in the synthesis of ethyl lactate

Entry	Catalyst	Calc. T (°C)	Y_{EL} (%)	X_{DHA} (%)	Sel. $_{EL}$ (%)	TON[c]
1	Sn-2-F127	250	46	62	76	127
2	Sn-5-F127	250	50	65	76	125
3	Sn-5-F127[a]	250	89	89	≥99	45
4	Sn-0-F127[b]	550	22	37	60	67
5	Sn-0-F127[b]	250	28	43	65	76
6	Sn-2-F127	550	30	51	59	104
7	Sn-MCM-41[23]	550	30	32	94	37
8	Sn-MCM-41[a,23]	550	98	100	98	30

Reaction conditions: 50 mg of catalyst, 5 mL of 0.4 M DHA solution in absolute ethanol, 6 h at 90 °C under 1200 rpm stirring. A "time analysis" is provided for Sn-5-F127 (entry 2) in Figure S8. [a] 200mg of catalyst, 5 mL of 0.4 M DHA solution in absolute ethanol, 24h at 90 °C under 1200 rpm stirring, [b] Non-methylated material synthesized in the same condition as Entry 1-2. [c] TON (Turnover number) here defined as mol of DHA converted / mol of Sn after 6 hours of reaction.

However, the comparison between the methylated samples and the non-methylated reference catalyst (Sn-0-F127) should be made with care. Indeed, the methylated catalysts were calcined at 250°C, while the non-methylated solid was directly calcined at 550°C as in our previous works (entry 4, table 3). So, an

additional test was performed after calcining the Sn-0-F127 material at 250 °C (entry 5, table 3). Only a minor difference was observed in terms of catalytic activity (compare entries 4 and 5, table 3), strengthening the positive results obtained with methylated silicates. As a countercheck, a significant loss of activity was observed when testing Sn-2-F127 (entry 6) after a thermal treatment at 550 °C where a complete removal of the methyl-functionalization is expected. It is relevant to highlight that the calcination may affect also the physicochemical properties of the materials such as surface area and surface hydroxyl content. For this reason, to even better isolate and evidence the influence of the surface methylation the activity of Sn-0-F127 (entries 5 and 6) and of Sn-2-F127 (entries 1 and 6) was normalized with the surface area both after calcination at 250°C and 550°C (Figure S9). From this analysis, the catalyst Sn-2-F127 again emerged as the most active when the surface methylation is preserved at 250 °C. From a direct comparison with an active catalyst reported in literature (table 3), the methylated solids displayed better performances in terms of TON under the same reaction conditions (compare entries 2 and 3 with entries 7 and 8). Increasing the catalyst/reactant ratio, it is possible to push the reaction to almost full conversion of DHA and to achieve a 99% EL selectivity owing to the reversible formation of the intermediate.

To further support the importance of the methylation on the ethyl lactate yield, different thermal treatments at increasing temperature were performed on both Sn-2-F127 and Sn-5-F127 (figure 5). A progressive decrease in the catalytic activity of the solids was observed with increasing calcination temperature which can be related to the progressive removal of the organic functionalities.

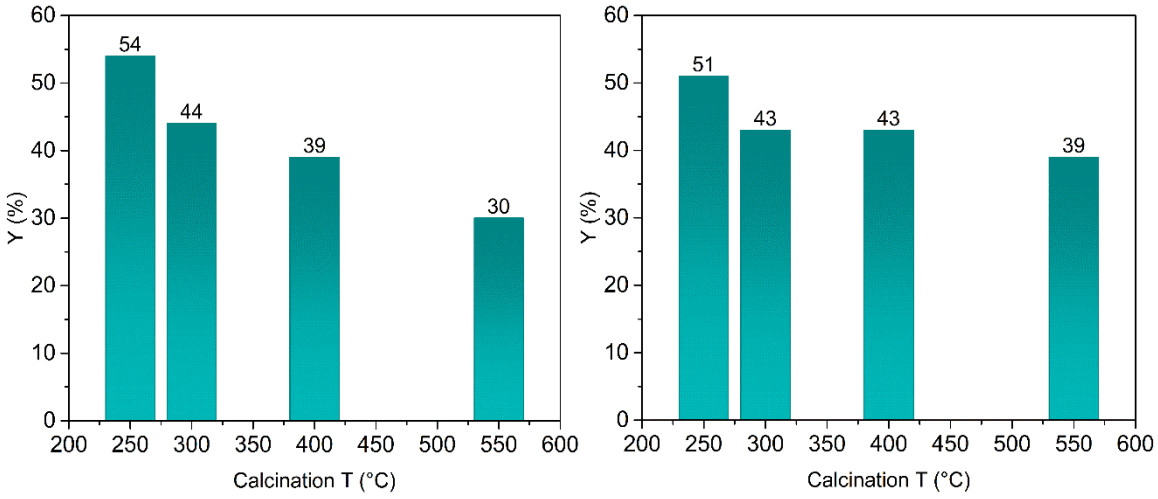

Figure 5. Influence of the calcination temperature on the activity of Sn-2-F127 (left) and Sn-5-F127 (right) catalysts. Reaction conditions: 50 mg of catalyst, 5 mL of 0.4 M DHA solution in absolute ethanol, 6 h at 90 °C.

The enhanced activity of the methylated materials could be ascribed to the lower interaction of water with the more hydrophobic surface of the catalysts. Water molecules represent the side product of the synthesis of EL (scheme 1). As previously discussed, the local removal of water in proximity of the active sites would shift the dehydration equilibrium through the formation of the PA intermediate with a consequent increase of the overall EL yield. However, at relatively high methylation degrees, surface methylation seemed to have a detrimental effect, possibly related to the fact that a lower proportion of Sn sites are available at the surface or that the adsorption of a hydrophilic substrate such as DHA is hindered. A good compromise is, hence, achieved in presence of Sn-5-F127 which displays a relatively low methylation degree. These results further support the importance of a precise tuning of the hydrophobic/hydrophobic balance of the catalyst surface.[28,47]

The excellent activity of the Sn-5-F127 catalyst was further evidenced with a quantitative experiment. Increasing the catalyst/reactant ratio (See experimental), an almost full conversion of DHA was achieved at 90 °C after 24 h of reaction, together with a 92% EL selectivity. This experiment was also selected to evaluate the sustainability of our ethyl lactate production process. After reaction, the catalyst was removed by centrifugation and the solvent was recovered through distillation. The E-factor was calculated following the formula: E-factor = [(0.360g DHA + 7.8g EtOH – 6.2g EtOH {recovered by distillation} – 0.418g EL) / 0.418g EL] = 3.7. The efficient separation and reuse of the heterogeneous catalyst as well as the possibility to easily recover the reaction solvent result in a very low waste production protocol presenting a promisingly low E-factor.

When working in heterogeneous conditions, conversion, TON and selectivity do not represent the only parameters that should be considered. A key role is played by the stability of the catalyst under the reaction conditions which determines the possibility to reuse it in multiple catalytic cycles, or to envisage

the design of a continuous flow process. The reusability of the Sn-5-F127 solid was investigated in consecutive runs (Figure 6). After each cycle the catalyst was separated via filtration from the reaction mixture, washed and thermally regenerated. From this study emerged that the good selectivity of the catalyst was preserved with the cycles, while the activity suffered of a slight decrease after the first run followed by a stabilization of the catalytic performances. The initial activity drop is not ascribed to a partial removal of the Me groups that would occur during regeneration since ^{29}Si solid state MAS NMR spectroscopy revealed a constant proportion of methylated moieties even after the 4th reaction (see Figure S10). Hence, it is put forward that the decrease in EL yield after the first cycle is linked to the adsorption of organic species at the material surface. It is indeed known from the literature[48] that a full regeneration of similar stannosilicate materials can be achieved with a thermal treatment at higher temperature (>300°C), which would however not be applicable in the present case as the methyl groups have to be preserved.

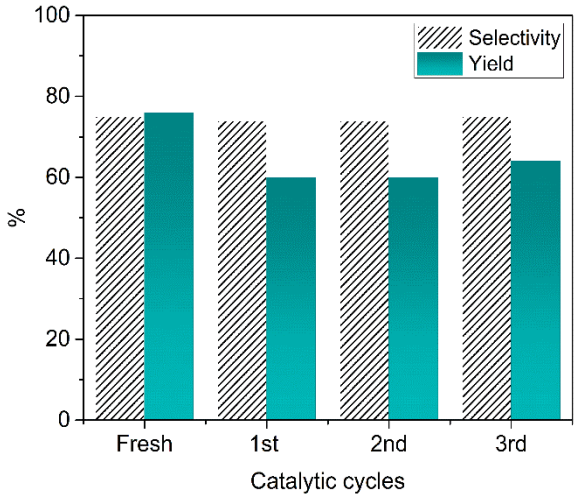

Figure 6. Recycling test of Sn-5-F127. Conditions: 100mg of catalyst, 100mg of DHA in 5mL EtOH, 3h at 90°C

In order to further prove that the activity is solely due to the solid, a hot filtration test was performed on Sn-5-F127. After 1 h of reaction, the conversion of DHA was evaluated and the catalyst was removed via hot filtration. The filtrate was further allowed to react for 5 h in the absence of the catalyst. The conversion

remained unchanged (Figure 7), indicating the absence of leaching of active sites and thus the stability of the incorporated metal sites under the selected reaction conditions.

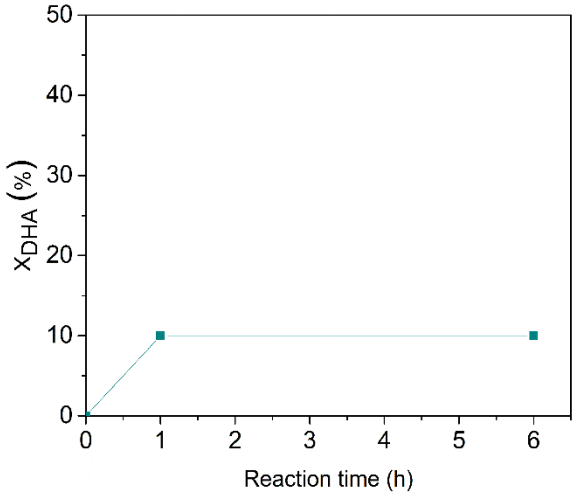

Figure 7. Hot filtration with Sn-5-F127 as catalyst. DHA conversion after 1h and 6h (catalyst removed).

Conclusions

The aerosol-assisted sol-gel process was implemented to synthesize a series of Sn-silicates with different degrees of methylation in a co-synthetic approach. A simple procedure for the effective removal of the surfactant was optimized using a mild calcination treatment. The materials displayed promising characteristics for catalytic applications such as controlled mesoporosity, high surface area and narrow particles size distribution. A successful dispersion Sn within the silica framework was confirmed via ^{119}Sn solid state NMR, which showed the presence single site Sn in tetrahedral coordination. Moreover, ^{29}Si and ^{13}C solid-state MAS (magic-angle-spinning) NMR experiments revealed a degree of methylation close to the theoretical value, hence proving the efficacy of the adopted procedure. Methylated Sn-silicates were tested in the conversion of dihydroxyacetone to ethyl lactate and a positive influence of the methylation on the performances of all the catalysts in terms of both activity and selectivity compared to the non-methylated solid was proved. Furthermore, it was observed that even a very low degree of methylation (i.e. 2%) is effective to enhance the catalytic performance of the materials. In particular, the best results were

obtained with the solids synthesized using F127 as templating agent. The stability of the catalysts against leaching under the selected reaction conditions was proved by a hot filtration test. Moreover, the best catalyst was successfully used and recycled several times and showed stable activity levels.

Experimental Section

Materials

Pluronic® P-123, Pluronic® F127, Hydrochloric acid (37%), tetraethyl orthosilicate (TEOS purity ≥99.99%), methyltriethoxysilane (MTES) and tin (IV) chloride pentahydrate ($SnCl_4 \cdot 5H_2O$ purity 98.0%) were all purchased from Sigma–Aldrich. Absolute ethanol was purchased from Fisher Scientific (Analytical grade).

Catalyst preparation

Methyl-functionalized Sn-silicates (Sn-x) were synthesized from a mixture of two silica sources, TEOS and MTES and four degrees of functionalization have been selected: 2, 5, 10 and 30 $_{mol}$%. Pluronic F127 and P123 have been used as templating agents. Solution **1** was obtained by hydrolyzing MTES and TEOS in an HCl, 0.02 M aqueous solution (20 g). Solution **2** was prepared by dissolving Pluronic® P123 or F127 (3.9 g) in ethanol (45 g) and acid aqueous solution (HCl, 0.02 M, 8 g). Solutions **1** and **2** were left stirring overnight at room temperature. Then tin (IV) chloride ($SnCl_4 \bullet 5H_2O$) was added to solution **1** in order to reach a Si/Sn molar ratio of 74. Solutions **1** and **2** were mixed together and further stirred at room temperature for 30 minutes. The clear solution obtained was atomized with a 6-Jet 9306A atomizer (TSI). The aerosol droplets were dried by passing through a tubular furnace set at 350 °C. The dried powders were collected on an absolute filter (cellulose nitrate), dried at 80°C for one night and then calcined at the selected temperature (heating rate of 1 °C/min) under static air.

Characterization

Transmission electron microscopy (TEM) was performed using a Philips Tecnai 10 microscope operating at 80 kV. Nitrogen physisorption analyses were carried out at 77 K with a Micromeritics Tristar 3000. Prior to the analysis, the samples were pre-treated overnight at 150 °C under reduced pressure (0.1 mbar). The Brunauer–Emmet–Teller (BET) method was applied in the 0.05-0.30 P/P_0 range to calculate the specific

surface area. Pore size distribution was calculated from the adsorption isotherm using the Barrett–Joyner–Halenda (BJH) method. Powder X-ray diffraction (XRD) patterns were recorded on a PANalytical X'pert diffractometer with Cu Kα radiation (k = 1.54178 Å). Elemental analysis was done by Inductively coupled plasma optical emission spectroscopy, using an Optima 8000 ICP-OES Spectrometer. The Si environment and the coordination of the Sn atoms were studied by ^{29}Si MAS-NMR and static ^{119}Sn NMR.

^{29}Si NMR spectra were recorded on a Bruker Avance-500 spectrometer operating at 11.7 T (99.3 MHz for ^{29}Si) using a 4mm CP-MAS Bruker probe (at room temperature). The sample was packed in a 4 mm zirconia rotor and measured with a spinning frequency of 8000 Hz. Quantitative ^{29}Si spectra were recorded using a 300s relaxation delay, a 3µs (90°) excitation pulse, and a 52 ms acquisition time. CP-MAS spectra were recorded using a 5 s relaxation delay and 5 ms contact time. The processing comprised exponential multiplication of the FID with a line broadening factor of 30 Hz, zero-filling, Fourier transform, phase and baseline corrections. The chemical shift scale was calibrated at room temperature using solid 3-(Trimethylsilyl)-1-propanesulfonic acid sodium salt (DSS) as a reference (0.0 ppm). ^{13}C NMR spectra were recorded at a spinning frequency of 8000Hz. CP-MAS spectra were recorded using a 5s relaxation delay and 2ms contact time.

^{119}Sn NMR spectra were obtained at room temperature on a Varian VNMRS-400 spectrometer operating at 9.4 T (149 MHz for ^{119}Sn) using a 5mm wideline probe. The sample was packed in a 5 mm glass tube and studied in static condition. ^{119}Sn spectra were recorded using the Hahn echo pulse sequence with a 60s relaxation delay, a 1.5µs (90°) excitation pulse, and a 5 ms acquisition time. The processing comprised exponential multiplication of the FID with a line broadening factor of 1000 Hz, zero-filling, Fourier transform, phase and baseline corrections. The chemical shift scale was calibrated using the isotropic shift of SnO_2 (-603 ppm) at room temperature.[49,50]

Production of ethyl lactate from dihydroxyacetone and E-factor calculation

Batch catalytic reactions were performed in a capped vial. 180 mg of DHA (in the form of 1,3-dihydroxyacetone dimer) and 25 mg of decane (0.19 mmol, as GC internal standard) were dissolved in 3.92 g of absolute ethanol (used both as solvent and reactant) at 45 °C for 30 min. Then, the selected amount of

catalyst was added to the solution at room temperature. The reaction mixture was heated at 90 °C under stirring (1200 rpm). After a selected reaction time, the catalyst was separated by centrifugation and the solution was analyzed by gas chromatography (Trace GC Ultra, Interscience). The quantification of pyruvaldehyde diethylacetal was made using the same response factor as for ethyl lactate. Under these conditions, considering that no other by-products were present, the total carbon balance was always very close to 100 %. For recycling tests, the catalyst was separated from the reaction mixture by centrifugation followed by sonication in ethanol (5 x 10mL). The catalyst was finally calcined in air at 300 °C for 4h (heating rate 1 °C/ min). In the leaching tests the catalyst was removed by centrifugation from the reaction mixture after 1h and the mixture was further reacted for another 5h. The products were analyzed after 1 h and 6 h. For the E-factor calculation a quantitative test was performed at 24h using 200mg of catalyst, 0.360g of DHA in 7.8g of absolute ethanol. At the end of the reaction, the catalyst was removed by centrifugation and ethanol was recovered by distillation. The EL isolate yield used for the E factor estimation was obtained via GC analysis.

Acknowledgements

Authors acknowledge the 'Communauté française de Belgique' for the financial support – including the PhD fellowship of A. Vivian – through the ARC programme (15/20-069). This research used resources of the nuclear magnetic resonance service located at the University of Namur. This service is a member of the "Plateforme Technologique Physico-Chemical Characterization" – PC^2. François Devred is thanked for the technical and logistical support.

Supporting Information.

Additional ^{29}Si MAS NMR, ^{119}Sn Static solid state NMR and ^{13}C MAS NMR spectra; calculated degree of methylation; attempted solvent extraction procedures; full characterization of Sn-10-F127, Sn-30-F127, Sn-0-F127; time analysis on the conversion of DHA to EL using Sn-5-F127; activity normalized by surface area; characterization of spent catalyst.

References

(1) Anastas, P. T.; Warner, J. C. 12 Principles of Green Chemistry. Green Chemistry: Theory and Practice. Oxford Univ. Press New York, By Permis. Oxford Univ. Press 1998.

(2) Erythropel, H. C.; Zimmerman, J. B.; de Winter, T. M.; Petitjean, L.; Melnikov, F.; Lam, C. H.; Lounsbury, A. W.; Mellor, K. E.; Janković, N. Z.; Tu, Q.; et al. The Green ChemisTREE: 20 Years after Taking Root with the 12 Principles. *Green Chem.* **2018**, *20* (9).

(3) De Bhowmick, G.; Sarmah, A. K.; Sen, R. Lignocellulosic Biorefinery as a Model for Sustainable Development of Biofuels and Value Added Products. *Bioresour. Technol.* **2018**, *247*, 1144–1154.

(4) Zhou, C.-H.; Xia, X.; Lin, C.-X.; Tong, D.-S.; Beltramini, J. Catalytic Conversion of Lignocellulosic Biomass to Fine Chemicals and Fuels. *Chem. Soc. Rev.* **2011**, *40* (11), 5588-5617.

(5) Corma, A.; Iborra, S.; Velty, A. Chemical Routes for the Transformation of Biomass into Chemicals. *Chem. Rev.* **2007**, *107* (6), 2411–2502.

(6) Drumright, R. E.; Gruber, P. R.; Henton, D. E. Polylactic Acid Technology. *Adv. Mater.* **2000**, *12* (23), 1841–1846.

(7) Sheldon, R. A. Green Solvents for Sustainable Organic Synthesis: State of the Art. *Green Chem.* **2005**, *7* (5), 267-278.

(8) Holm, M. S.; Saravanamurugan, S.; Taarning, E. Conversion of Sugars to Lactic Acid Derivatives Using Heterogeneous Zeotype Catalysts. *Science (80-.).* **2010**, *328* (5978), 602–605.

(9) Orazov, M.; Davis, M. E. Tandem Catalysis for the Production of Alkyl Lactates from Ketohexoses at Moderate Temperatures. *Proc. Natl. Acad. Sci.* **2015**, *112* (38), 11777–11782.

(10) Gross, R. A.; Kalra, B.; Bastoli, C.; Gross, R. A.; Gu, J.-D.; Eberiel, D.; McCarthy, S. P.; Buchanan, C. M.; Pearcy, B. G.; White, A. W.; et al. Biodegradable Polymers for the Environment. *Science* **2002**, *297*

(5582), 803–807.

(11) Lim, L.-T.; Auras, R.; Rubino, M. Processing Technologies for Poly(Lactic Acid). *Prog. Polym. Sci.* **2008**, *33* (8), 820–852.

(12) De Clercq, R.; Dusselier, M.; Makshina, E.; Sels, B. F. Catalytic Gas-Phase Production of Lactide from Renewable Alkyl Lactates. *Angew. Chemie - Int. Ed.* **2018**, *57* (12), 3074–3078.

(13) Dusselier, M.; Van Wouwe, P.; Dewaele, A.; Jacobs, P. A.; Sels, B. F. Shape-Selective Zeolite Catalysis for Bioplastics Production. *Science (80-.).* **2015**, *349* (6243), 78–80.

(14) Dusselier, M.; Van Wouwe, P.; Dewaele, A.; Makshina, E.; Sels, B. F. Lactic Acid as a Platform Chemical in the Biobased Economy: The Role of Chemocatalysis. *Energy Environ. Sci.* **2013**, *6* (5), 1415–1442.

(15) De Clercq, R.; Dusselier, M.; Poleunis, C.; Debecker, D. P.; Giebeler, L.; Oswald, S.; Makshina, E.; Sels, B. F. Titania-Silica Catalysts for Lactide Production from Renewable Alkyl Lactates: Structure-Activity Relations. *ACS Catal.* **2018**, 8 (9), 8130–8139**.**

(16) Mäki-Arvela, P.; Simakova, I. L.; Salmi, T.; Murzin, D. Y. Production of Lactic Acid/Lactates from Biomass and Their Catalytic Transformations to Commodities. *Chem. Rev.* **2014**, *114* (3), 1909–1971.

(17) Sheldon, R. A. Metrics of Green Chemistry and Sustainability: Past, Present, and Future. *ACS Sustain. Chem. Eng.* **2018**, *6* (1), 32–48.

(18) Hayashi, Y.; Sasaki, Y. Tin-Catalyzed Conversion of Trioses to Alkyl Lactates in Alcohol Solution. *Chem. Commun.* **2005**, 21, 2716–2718.

(19) Osmundsen, C. M.; Holm, M. S.; Dahl, S.; Taarning, E. Tin-Containing Silicates: Structure-Activity Relations. *Proc. R. Soc. A Math. Phys. Eng. Sci.* **2012**, *468* (2143), 2000–2016.

(20) Tosi, I.; Riisager, A.; Taarning, E.; Jensen, P. R.; Meier, S. Kinetic Analysis of Hexose Conversion to Methyl Lactate by Sn-Beta: Effects of Substrate Masking and of Water. *Catal. Sci. Technol.* **2018**, 8,

2137-2145.

(21) Pescarmona, P. P.; Janssen, K. P. F.; Delaet, C.; Stroobants, C.; Houthoofd, K.; Philippaerts, A.; De Jonghe, C.; Paul, J. S.; Jacobs, P. a.; Sels, B. F. Zeolite-Catalysed Conversion of C3 Sugars to Alkyl Lactates. *Green Chem.* **2010**, *12* (6), 1083–1089.

(22) Taarning, E.; Saravanamurugan, S.; Holm, M. S.; Xiong, J.; West, R. M.; Christensen, C. H. Zeolite-Catalyzed Isomerization of Triose Sugars. *ChemSusChem* **2009**, *2* (7), 625–627.

(23) Li, L.; Stroobants, C.; Lin, K.; Jacobs, P. A.; Sels, B. F.; Pescarmona, P. P. Selective Conversion of Trioses to Lactates over Lewis Acid Heterogeneous Catalysts. *Green Chem.* **2011**, *13* (5), 1175.

(24) Li, L.; Collard, X.; Bertrand, A.; Sels, B. F.; Pescarmona, P. P.; Aprile, C. Extra-Small Porous Sn-Silicate Nanoparticles as Catalysts for the Synthesis of Lactates. *J. Catal.* **2014**, *314*, 56–65.

(25) De Clippel, F.; Dusselier, M.; Van Rompaey, R.; Vanelderen, P.; Dijkmans, J.; Makshina, E.; Giebeler, L.; Oswald, S.; Baron, G. V.; Denayer, J. F. M.; et al. Fast and Selective Sugar Conversion to Alkyl Lactate and Lactic Acid with Bifunctional Carbon-Silica Catalysts. *J. Am. Chem. Soc.* **2012**, *134* (24), 10089–10101.

(26) Godard, N.; Collard, X.; Vivian, A.; Bivona, L. A.; Fiorilli, S.; Fusaro, L.; Aprile, C. Rapid Room Temperature Synthesis of Tin-Based Mesoporous Solids: Influence of the Particle Size on the Production of Ethyl Lactate. *Appl. Catal. A Gen.* **2018**, *556*, 73–80.

(27) Godard, N.; Vivian, A.; Fusaro, L.; Cannavicci, L.; Aprile, C.; Debecker, D. P. High-Yield Synthesis of Ethyl Lactate with Mesoporous Tin Silicate Catalysts Prepared by an Aerosol-Assisted Sol-Gel Process. *ChemCatChem* **2017**, *9 (12)*, 2211–2218.

(28) Lari, G. M.; Dapsens, P. Y.; Scholz, D.; Mitchell, S.; Mondelli, C.; Pérez-Ramírez, J. Deactivation Mechanisms of Tin-Zeolites in Biomass Conversions. *Green Chem.* **2016**, *18* (5), 1249–1260.

(29) Debecker, D. P.; Le Bras, S.; Boissière, C.; Chaumonnot, A.; Sanchez, C. Aerosol Processing: A Wind of

Innovation in the Field of Advanced Heterogeneous Catalysts. *Chem. Soc. Rev.* **2018**, *47*, 4112-4155.

(30) Pega, S.; Boissière, C.; Grosso, D.; Azaïs, T.; Chaumonnot, A.; Sanchez, C. Direct Aerosol Synthesis of Large-Pore Amorphous Mesostructured Aluminosilicates with Superior Acid-Catalytic Properties. *Angew. Chemie - Int. Ed.* **2009**, *48* (15), 2784–2787.

(31) Debecker, D. P.; Stoyanova, M.; Colbeau-Justin, F.; Rodemerck, U.; Boissière, C.; Gaigneaux, E. M.; Sanchez, C. One-Pot Aerosol Route to MoO_3-SiO_2-Al_2O_3 Catalysts with Ordered Super Microporosity and High Olefin Metathesis Activity. *Angew. Chemie - Int. Ed.* **2012**, *51* (9), 2129–2131.

(32) Maksasithorn, S.; Praserthdam, P.; Suriye, K.; Debecker, D. P. Preparation of Super-Microporous WO_3-SiO_2 Olefin Metathesis Catalysts by the Aerosol-Assisted Sol-Gel Process. *Microporous Mesoporous Mater.* **2015**, *213*, 125–133.

(33) Debecker, D. P.; Stoyanova, M.; Rodemerck, U.; Colbeau-Justinc, F.; Boissère, C.; Chaumonnot, A.; Bonduelle, A.; Sanchez, C. Aerosol Route to Nanostructured WO_3-SiO_2-Al_2O_3 Metathesis Catalysts: Toward Higher Propene Yield. *Appl. Catal. A Gen.* **2014**, *470*, 458–466.

(34) Sachse, A.; Hulea, V.; Kostov, K. L.; Marcotte, N.; Boltoeva, M. Y.; Belamie, E.; Alonso, B. Efficient Mesoporous Silica–titania Catalysts from Colloidal Self-Assembly. *Chem. Commun.* **2012**, *48* (86), 10648.

(35) Guo, Z.; Xiong, G.; Liu, L.; Li, P.; Hao, L.; Cao, Y.; Tian, F. Aerosol-Assisted Synthesis of Hierarchical Porous Titanosilicate Molecular Sieve as Catalysts for Cyclohexene Epoxidation. *J. Porous Mater.* **2016**, *23* (2), 407–413.

(36) Boissiere, C.; Grosso, D.; Chaumonnot, A.; Nicole, L.; Sanchez, C. Aerosol Route to Functional Nanostructured Inorganic and Hybrid Porous Materials. *Adv. Mater.* **2011**, *23* (5), 599–623.

(37) Debecker, D. P. Innovative Sol-Gel Routes for the Bottom-up Preparation of Heterogeneous Catalysts. *Chem. Rec.* **2018**, *18*, 662–675.

(38) Zhang, F.; Kang, C.; Wei, Y.; Li, H. Aerosol-Spraying Synthesis of Periodic Mesoporous Organometalsilica Spheres with Chamber Cavities as Active and Reusable Catalysts in Aqueous Organic Reactions. *Adv. Funct. Mater.* **2011**, *21* (16), 3189–3197.

(39) Gholampour, N.; Chaemchuen, S.; Hu, Z. Y.; Mousavi, B.; Van Tendeloo, G.; Verpoort, F. Simultaneous Creation of Metal Nanoparticles in Metal Organic Frameworks via Spray Drying Technique. *Chem. Eng. J.* **2017**, *322*, 702–709.

(40) Kruk, M.; Jaroniec, M.; Ko, C. H.; Ryoo, R. Characterization of the Porous Structure of SBA-15. *Chem. Mater.* **2000**, *12* (7), 1961–1968.

(41) Grudzien, R. M.; Jaroniec, M. Cage-like Ordered Silica with Large Mesopore Volume Synthesized by Doubling Amount of Polymer, Adding Sodium Chloride and Lowering Acid Concentration. *Chem. Commun.* **2005**, 8, 1076–1078.

(42) Zhao, L.; Zhu, G.; Zhang, D.; Di, Y.; Chen, Y.; Terasaki, O.; Qiu, S. Synthesis and Structural Identification of a Highly Ordered Mesoporous Organosilica with Large Cagelike Pores. *J. Phys. Chem. B* **2005**, *109* (2), 764–768.

(43) Grudzien, R. M.; Grabicka, B. E.; Jaroniec, M. Effective Method for Removal of Polymeric Template from SBA-16 Silica Combining Extraction and Temperature-Controlled Calcination. *J. Mater. Chem.* **2006**, *16* (9), 819–823.

(44) Xu, R.; Pang, W.; Yu, J.; Huo, Q.; Chen, J. *Chemistry of Zeolites and Related Porous Materials: Synthesis and Structure*; Wiley, 2010.

(45) Prouzet, E. Assembly of Mesoporous Molecular Sieves Containing Wormhole Motifs by A. *Angew. Chemie Int. Ed.* **1997**, *36*, 516–518.

(46) Rama Rao, G. V.; López, G. P.; Bravo, J.; Pham, H.; Datye, A. K.; Xu, H. F.; Ward, T. L. Monodisperse Mesoporous Silica Microspheres Formed by Evaporation-Induced Self Assembly of Surfactant

Templates in Aerosols. *Adv. Mater.* **2002**, *14* (18), 1301–1304.

(47) Li, L.; Cani, D.; Pescarmona, P. P. Metal-Containing TUD-1 Mesoporous Silicates as Versatile Solid Acid Catalysts for the Conversion of Bio-Based Compounds into Valuable Chemicals. *Inorganica Chim. Acta* **2015**, *431*, 289–296.

(48) Collard, X.; Li, L.; Lueangchaichaweng, W.; Bertrand, A.; Aprile, C.; Pescarmona, P. P. Ga-MCM-41 Nanoparticles : Synthesis and Application of Versatile Heterogeneous Catalysts. *Catal. Today* **2014**, *235*, 184–192.

(49) Cossement, C.; Darville, J.; Gilles, J.; Nagy, J. B. Chemical Shift Anisotropy and Indirect Coupling in SnO_z and SnO. *Magn. Reson. Chem.* **1992**, 30, 263–270.

(50) Aliev, A. E.; Bartók, A. P.; Yates, J. R. Tin Chemical Shift Anisotropy in Tin Dioxide: On Ambiguity of CSA Asymmetry Derived from MAS Spectra. *Solid State Nucl. Magn. Reson.* **2018**, *89*, 1–10.

TOC/Abstract graphic

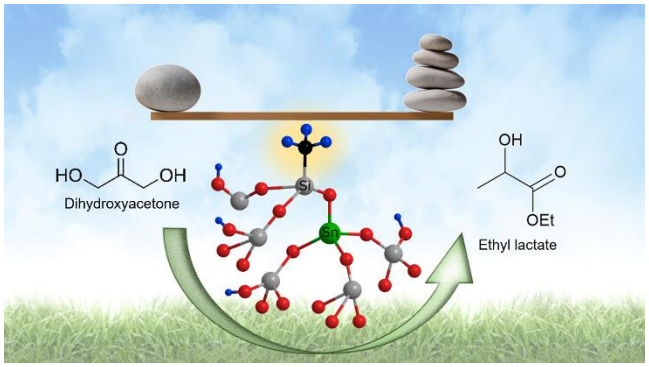

A one-pot aerosol route allows introducing hydrophobicity on the surface of mesoporous stannosilicate catalysts, resulting in improved catalytic performance in the synthesis of ethyl lactate